

RESEARCH ARTICLE

# Attenuation of early liver fibrosis by pharmacological inhibition of smoothed receptor signaling

Akshay Pratap<sup>1,\*</sup>, Saurabh Singh<sup>2</sup>, Vaibhav Mundra<sup>2</sup>, Ningning Yang<sup>2</sup>, Ravikiran Panakanti<sup>2</sup>, James D Eason<sup>1</sup>, and Ram I Mahato<sup>2</sup>

<sup>1</sup>Division of Solid Organ Transplantation, Methodist University Hospital, Memphis, TN, USA and <sup>2</sup>Department of Pharmaceutical Sciences, University of Tennessee Health Sciences Center, Memphis, TN, USA

## Abstract

Hedgehog (Hh) signaling is involved in the pathogenesis of liver fibrosis. It has been previously shown that Hh-inhibitor cyclopamine (CYA) can reduce liver fibrosis in rats. However, CYA is not stable *in vivo*, which limits its clinical application. This study compares the antifibrotic potential of two known Hh antagonists, vismodegib (GDC-0449, abbreviated to GDC) and CYA. GDC is a synthetic molecule presently in clinical cancer trials and has been reported to be safe and efficacious. These drugs attenuated early liver fibrosis in common bile duct ligated rats, improved liver function, and prevented hepatic stellate cell (HSC) activation, thereby suppressing epithelial to mesenchymal transition (EMT). While both CYA and GDC increased the number of proliferating cell nuclear antigen positive liver cells *in vivo*, only CYA increased Caspase-3 expression in HSCs in rat livers, suggesting that while GDC and CYA effectively attenuate early liver fibrosis, their hepatoprotective effects may be mediated through different modes of action. Thus, GDC has the potential to serve as a new therapeutic agent for treating early liver fibrosis.

**Keywords:** Hedgehog signaling, liver fibrosis, cyclopamine, GDC 0049, therapy

## Introduction

Chronic liver injury causes excessive accumulation of extracellular matrix (ECM), resulting in fibrosis, which if not treated in early phase, can lead to liver failure. Progression of liver fibrosis involves the activation of various cell types, including hepatocytes, bile ductular cells (cholangiocytes) and hepatic stellate cells (HSCs), which overproduce hedgehog (Hh) signaling ligands in response to liver injury (Chen et al., 2002). Regardless of the cell type involved in producing these ligands, HSCs are the major population responsible for liver repair and collagen production. Upon injury-mediated activation, HSCs acquire a myofibroblastic phenotype and produce excessive amounts of ECM, including type I collagen (Friedman, 2008; Sicklick et al., 2005). Several lines of evidence implicate the Hh signaling

pathway in this process (Choi et al., 2010a, Choi et al., 2010b, Omenetti et al., 2008; Omenetti et al., 2007). Hh ligands are soluble factors that interact with the plasma membrane-spanning receptor, Patched (Ptch), to de-repress the downstream intracellular signaling intermediate, Smoothed (Smo). Smo-initiated signals, in turn, activate Glioblastoma (Gli)-family transcription factors to induce expression of Hh-responsive genes that regulate target cell proliferation, viability and differentiation (Hooper and Scott, 2005). Hh signaling regulates remodeling of various adult tissues, including the nervous system, skin, heart, lung, and gastrointestinal tract. During embryogenesis and carcinogenesis, Hh ligands function as morphogens by modulating both mesendodermal fate and epithelial to mesenchymal transitions (EMT) (Varnat et al., 2009; Park

Akshay Pratap and Saurabh Singh contributed equally to this work.

\*Current address: Department of Surgery, University of Colorado, Denver, Colorado 80204, USA

Address for Correspondence: Dr. Ram I Mahato, Department of Pharmaceutical Sciences, University of Tennessee Health Sciences Center, 19 South Manassas, CRB RM224, Memphis, TN 38103-3303, USA. Tel: (901)448-6929. Fax: (901)448-2099.  
E-mail: rmahato@uthsc.edu; <http://www.uthsc.edu/pharmacy/rmahato>

(Received 09 July 2012; revised 07 August 2012; accepted 07 August 2012)

et al., 2010; Krull, 2010; Wang et al., 2010; Dormoy et al., 2009; Asaoka et al., 2010).

Hh signaling regulates liver injury during ischemia reperfusion (IR) of cholestatic liver induced by common bile duct ligation (CBDL) in a rat model, and inhibition of Hh pathway by preconditioning with Smo inhibitor cyclopamine (CYA) confers hepatoprotection (Thayer et al., 2003; Marshall, 2006). Since CYA is acid-labile and converts to non-effective derivatives, we decided to compare its efficacy with a more stable small molecule inhibitor vismodegib (GDC-0449, abbreviated as GDC), which has prolonged plasma half-life (Tremblay et al., 2008). GDC has recently been shown to have a safe profile in phase I clinical trials for treating solid organ tumors (Lorusso et al., 2011). To this end, expression of Hh ligands and inhibition of Hh pathway by treatment with GDC was evaluated in the rat liver with early stages of CBDL-mediated fibrosis. Results show that GDC, such as CYA, can ameliorate early fibrosis in a rat model of CBDL and is more effective in attenuating liver injury than CYA. A decrease in tissue damage was observed that correlated to suggest the intriguing possibility that while CYA and GDC inhibit Hh signaling by antagonizing Smo receptor, their downstream mechanisms of action through which early liver fibrosis is attenuated, may be different. Further studies are thus required to explore these mechanisms.

## Materials and methods

### Chemicals and antibodies

CYA and GDC were purchased from LC Laboratories (Woburn, MA). SYBR Green real-time PCR master mix and reverse transcription reagents were purchased from Applied Biosystems (Foster city, CA). Goat anti-rabbit Shh, Gli-1, Ptch-1 primary antibodies were purchased from Santa Cruz Biotechnology (Santa Cruz, CA) while type I collagen primary antibody was from Novus (Littleton, CO). Goat  $\alpha$ -smooth muscle actin ( $\alpha$ -SMA) antibody was purchased from Abcam (Cambridge, MA). Mouse proliferating cell nuclear antigen (PCNA) monoclonal antibody (Clone IPO-38) was purchased from Cayman Chemical Company (Ann Arbor, MI). Goat anti-rabbit Alexa Fluor 488 and Alexa Fluor 594, rabbit anti-goat Alexa Fluor 488 and goat anti-mouse 594 secondary antibodies and 4', 6-diamidino-2-phenylindole (DAPI) were purchased from Invitrogen (Carlsbad, CA). All other chemicals were purchased from Sigma-Aldrich (St. Louis, MO), unless otherwise noted.

### Animal experiments

Animal studies were approved by the Animal Care and Use Committee (ACUC) of the University of Tennessee. Sprague-Dawley rats were housed with 12h light-dark cycles and with water and standard rat chow ad libitum. Animal experiments were performed as per the NIH (<http://grants1.nih.gov/grants/olaw/references/phspol>.

htm) guidelines and protocols. Isoflurane was used to anesthetize rats.

### Common bile duct ligation and animal groups

Biliary fibrosis was induced in adult Sprague-Dawley rats, weighing 230–250 g (Charles River), by CBDL as described (Ezure et al., 2000). On the day of CBDL, animals were divided into four groups: (i) sham (midline abdominal incision and closure) + vehicle ( $n = 4$ ), (ii) CBDL + vehicle ( $n = 8$ ), (iii) CBDL + CYA at 10 mg/kg/day ( $n = 5$ ), and (iv) CBDL + GDC at 10 mg/kg/day ( $n = 5$ ). GDC was formulated at 5 mg/ml concentration in 10% 2-hydroxypropyl- $\beta$ -cyclodextrin (HBCD) solution and stored at  $-40^{\circ}\text{C}$  till further use. GDC and CYA were administered via intraperitoneal injection every day for 7 days. The vehicle group was identical to the treatment groups, but rats were administered only 10% solution of HBCD. Animals were killed under isoflurane anesthesia after 1 week by puncture of the right ventricle and exsanguination. Serum was collected for biochemical analyses and liver pieces were fixed in 10% neutral buffered formalin or snap frozen in liquid nitrogen for further analysis.

### Real-time RT-PCR

Shh, Ptch-1, Gli-1,  $\alpha$ -SMA, TGF- $\beta$ , S100A4, E-cadherin, and collagen gene expression in rat livers was determined by real-time PCR as described earlier (Thayer et al., 2003) with some modifications (Singh et al., 2012). Briefly, total liver RNA was extracted and reverse transcribed to cDNA templates. In all, 100 ng of cDNA was amplified by real-time PCR using SYBR Green dye universal master mix on an LightCycler $^{\circledR}$ 480 (LC 480) (Applied Biosystems, Inc., Foster City, CA) using the primers for Shh (NCBI Accession# NM\_017221), Ptch-1 (NCBI Accession#; NM\_053566), Gli-1 (NCBI Accession# XM\_345832),  $\alpha$ -SMA (NCBI Accession# NP\_112266), S100A4 (NCBI Accession# NM\_05393v8), TGF- $\beta$ 1 (NCBI Accession# AAS554640), E-cadherin (NCBI Accession# NP\_112624), and  $\alpha$  (1) collagen (NCBI Accession # NP\_001128481). Following melting curve analysis, crossing point (Cp) was used for calculating the relative amount of mRNA compared with the house keeping gene, 18s and then scaled relative to controls, where control samples were set at a value of 1. Thus, results for all experimental samples were graphed as relative expression compared with the control.

### Liver biochemical function tests

Serum concentrations of aspartate aminotransferase (AST) and alanine aminotransferase (ALT), and total bilirubin were measured as indicators of hepatic injury using standard enzyme assay kits (ID Labs $^{\text{TM}}$  Inc, London, ON, Canada) and total bilirubin assay kit (Bio scientific, Austin, TX) according to the manufacturer's instructions.

### Quantification of hepatic collagen content

Hepatic collagen content was assessed by both morphometric analysis of Masson's trichrome staining of

liver tissue sections and hydroxyproline concentration. The area of positive Masson's trichrome staining was measured using UTHSC image tool software program. Hydroxyproline content was quantified colorimetrically from 0.2g liver samples as previously described (Panakanti et al., 2010). The results were expressed as micrograms of hydroxyproline per gram of liver.

### Liver histology

Liver samples were fixed in 10% buffered formalin, paraffin-embedded, and sectioned at 5  $\mu$ m. For standard histology, sections were stained with Hematoxylin-eosin (H&E) and Sirius red and then analyzed blindly as described previously (Marshall, 2006; Thayer et al., 2003).

### Immunofluorescent labeling

For immunolabeling, fresh snap frozen liver tissue samples were sectioned onto lysine coated slides. Sections were fixed in 95% ethanol for 5min and then air dried at room temperature for 24h. Briefly, slides were blocked with 10% goat serum, followed by overnight incubation with primary antibody at 4°C. Bound antibodies were developed with fluorescent secondary antibodies (Alexa Flour 488 or Alexa Flour 547). Nuclear staining was achieved using DAPI. Images were obtained on an inverted motorized microscope (Axiovert 200M, Zeiss) out-fitted with Cy5, Cy3, FITC, and DAPI filters. Three- and four-color images were captured using a Zeiss AxioCam, and pseudocolors assigned using Zeiss Axiovision software. The total number of PCNA-positive cells per slide was manually counted under light microscopy at 200 $\times$  magnification. In each slide, the total number of nuclei was also determined using a computer image analysis system (Image-1/Metamorph Imaging Systems, Universal Imaging Corporation, West Chester, PA). The ratio of PCNA-positive nuclei to the total number of nuclei X100 was used to obtain a PCNA index for each group.

### Western blot assay

Total protein was extracted by homogenizing liver tissues in radioimmunoprecipitation assay (RIPA) buffer containing protease inhibitor cocktail (Roche, Indianapolis, IN). The protein concentration was determined using a Bio-Rad RC DC protein assay kit (Hercules, CA). Proteins were resolved on 4–10% sodium dodecyl sulfate-polyacrylamide gel electrophoresis (SDS-PAGE) and subsequently transferred to Immobilonpolyvinylidene fluoride membrane using iBlot™ Dry Blotting System (Invitrogen, Carlsbad, CA). After blocking with 5% nonfat dry milk in 1  $\times$  PBST (PBS containing 0.05% Tween-20) for 1 h at room temperature, the membranes were incubated with  $\alpha$ -SMA, type 1 collagen or cyclin A primary antibodies for 16h at 4°C as described (Kepka-Lenhart et al., 1996). To correct for equal loading and blotting, all blots were re-probed with total actin antibody. Membrane was then incubated with horseradish peroxidase-conjugated anti-goat or anti-rabbit secondary antibody for 1h

at room temperature. Target proteins were detected by enhanced chemiluminescence detection kit (GE Healthcare Life Sciences, Pittsburgh, PA).

### Statistical analysis

All values in the figures and text were expressed as the mean  $\pm$  S.D. The results were analyzed and individual group means were compared with Student's unpaired *t*-test. A *p* value of at least 0.05 was considered statistically significant.

## Results

### SMO inhibitors preserve gross morphology and liver histology in CBDL rats

At the time of sacrifice, livers of control animals showed normal gross morphology, while CBDL rat livers were grossly enlarged and cholestatic with pitted surface. Treatment with CYA and GDC resulted in near normal liver morphology (Figure 1A, upper panels). Histological examination shows that normal liver had no fibrosis. CBDL also resulted in early periportal fibrosis around proliferating bile ducts, which was reduced by CYA and GDC treatment. Bile infarcts are confluent foci of hepatocyte feathery degeneration due to bile acid cytotoxicity and are a prominent feature of liver injury in the CBDL animals. Bile infarcts in the liver (indicated by arrows) were assessed by conventional H&E staining and quantified using digital image analysis. Histopathological examination of liver specimens demonstrated extensive bile infarcts in untreated CBDL rats. However, CYA and GDC treatment significantly reduced the extent and size of bile infarcts, suggesting that Smo inhibitors attenuate liver injury and protect tissue architecture in CBDL rats (Figure 1A, lower panels).

### SMO inhibitors attenuate liver injury following CBDL

Liver injury was examined by measuring serum AST, ALT, and total bilirubin concentrations, which were markedly increased in CBDL rats (Figure 1B). Values of these liver injury markers were significantly reduced in CYA and GDC-treated CBDL rats compared with untreated CBDL rats. GDC compared to CYA reduced the serum levels of ALT and bilirubin in a significant manner. However, no significant difference was observed in the extent of protection offered by GDC compared with CYA in serum AST levels.

### Upregulation of Hh pathway in CBDL rats

Compared to normal livers, Shh, Ptch-1, and Gli-1 transcripts were significantly upregulated in CBDL livers (Figure 2A). Treatment with CYA reduced gene expression significantly. GDC treatment similarly reduced the transcript expression. Compared to CYA, GDC was significantly more effective in downregulating Hh-ligand expression. Immunofluorescent staining for Gli-1 demonstrated not only a higher expression of Gli-1 in CBDL rats but also its presence in the nucleus as indicated

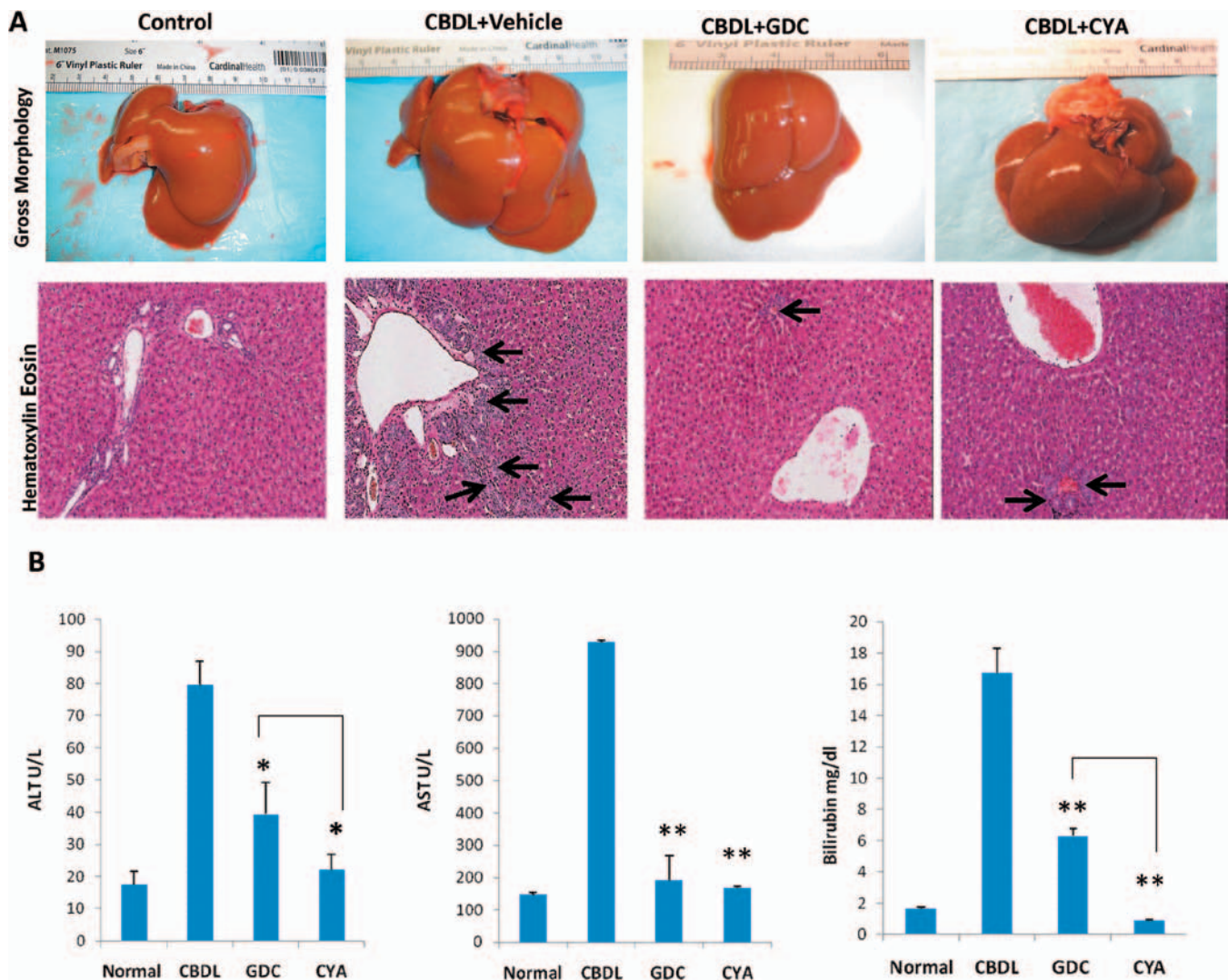


Figure 1. Morphological and histological evaluation of CBDL rat livers. (A) Top panels indicating distorted and pitted CBDL livers restored to near normal morphology following treatment with CYA (10 mg/kg) and GDC (5 mg/kg). Lower panels show H&E staining of liver specimens from sham controls and CBDL rats with or without treatment with CYA or GDC. Treatment with Smo inhibitors significantly ameliorated tissue damage and necrotic regions (arrows). (B) Treatment with Smo inhibitors preserves liver functions and reduces histological liver injury, including bile infarcts indicated by arrows. Serum AST, ALT and bilirubin in normal, vehicle treated CBDL, GDC-treated CBDL and CYA-treated CBDL rats were quantified. Serum markers in the Smo inhibitor treated groups were significantly lower than those in the vehicle treated group. Results are presented as the mean  $\pm$  S.D. ( $n = 4$ ); \* $p < 0.05$  and \*\* $p < 0.005$  compared to CBDL + vehicle treated rats.

by arrows. This translocation of Gli-1 was significantly reduced as a result of GDC treatment (indicated by arrows, merged panels, Figure 2B).

### SMO inhibitors attenuate EMT in CBDL rats

To understand the effect of Smo inhibitors on EMT in CBDL rats, expression levels of epithelial and mesenchymal markers in the liver tissue, such as  $\alpha$ -SMA, S100A4, TGF- $\beta$ 1, and E-cadherin, were determined by immunofluorescence (Figure 3A) and real-time PCR (Figure 3B), respectively. Treatment with CYA and GDC resulted in the restoration of epithelial genes, such as E-cadherin, and a downregulation of mesenchymal genes such as  $\alpha$ -SMA, S100A4, and TGF- $\beta$ 1. Immunofluorescence data indicate that CBDL rats had increased expression of mesenchymal markers in and around portal tracts

and biliary epithelial cells. Drug treatment increased E-cadherin preferentially in the lining of the bile ducts and portal tracts, suggesting that liver cells were possibly reacquiring an epithelial phenotype. Taken together, data suggest that GDC was more effective in restoring an epithelial phenotype in CBDL livers.

### SMO inhibitors induce liver cell proliferation in CBDL rats

Proliferation of liver cells is an adaptive physiologic response in hepatic diseases, and is a determinant of survival (Delhaye et al., 1996; Fang et al., 1994). However, in fibrotic livers, activated HSCs secrete inflammatory cytokines, Hh ligands and collagen and play an important role in etiology of liver fibrosis. Activation of HSCs following injury also results in damage to neighboring hepatocytes.

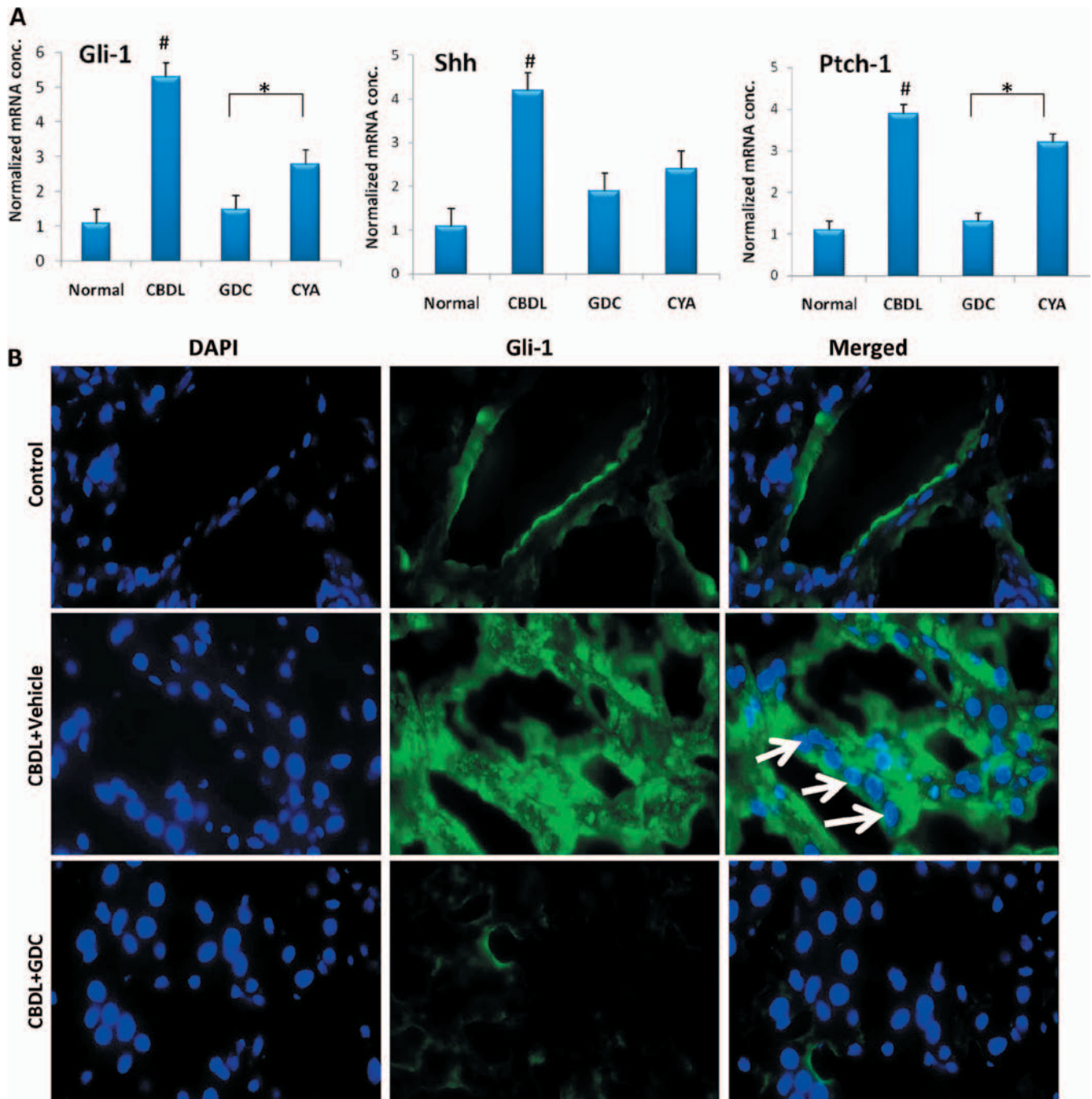


Figure 2. Hh pathway and ligand expression in livers of normal (control) and fibrotic rats. (A) Shh, Ptch-1 and Gli-1 expression in normal and CBDL rats quantified by real-time PCR after correction for the housekeeping gene 18s. CBDL treatment results in upregulation of Hh ligands. GDC treatment was more significantly effective in reducing Hh-ligand mRNA expression than CYA in CBDL livers. Indicated p values are calculated with respect to CBDL+ vehicle treated livers. (B) CBDL leads to enhanced Hh activity reflected as increased expression and nuclear translocation (arrows) of Gli-1 protein from cytoplasm. SMO inhibitors reduced expression and translocation of Gli-1 protein. Shown are representative images (original magnification,  $\times 100$ ).

To examine the possibility that Smo inhibitors preserve liver function by enhancing cellular proliferation following CBDL, protein expression for cyclin A in hepatic protein extracts (Figure 4A) and PCNA expression in liver specimens (Figure 4B) was assessed. Western blot analysis for proliferation marker cyclin A indicates higher protein expression in GDC-treated liver extracts compared to those treated with CYA. PCNA-positive nuclei in rat liver

sections were assessed by immunofluorescence staining and found to be increased in CYA and GDC-treated CBDL rats compared to vehicle-dosed CBDL rats. GDC treatment was more effective than CYA in inducing cellular proliferation and quantitative analysis indicates that on average, almost twice as many PCNA positive nuclei were counted in GDC-treated rat livers at high magnification compared to CYA-treated livers (Figure 4C).

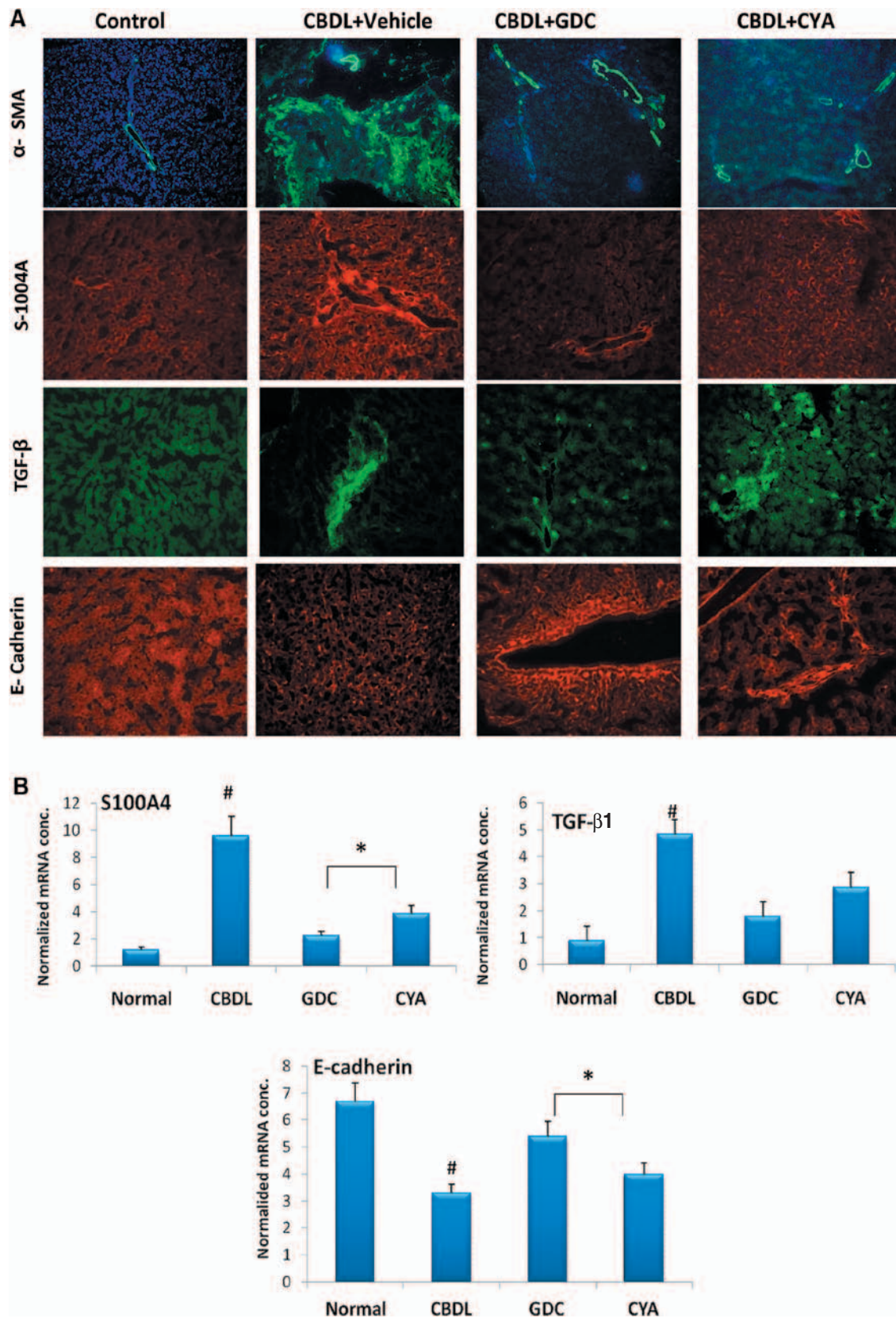


Figure 3. Smoothed (Smo) inhibitors attenuate EMT in CBDL rats. (A) Immunofluorescence staining was carried out to detect the expression of  $\alpha$ -SMA, S100A4, TGF $\beta$ 1, and E-cadherin in Smo inhibitor treated CBDL rats. The protein expression of  $\alpha$ -SMA, S100A4, and TGF $\beta$ 1 decreased significantly mainly around the fibrous septa. In parallel, enhanced upregulation of E-cadherin was observed on the endothelial surfaces of portal vein and periportal structures. Shown are representative images (original magnification,  $\times 40$ ). (B) Gene expression analysis of EMT markers in CBDL rats. Real-time RT-PCR was used to determine expression of EMT marker genes. GDC was more effective than CYA in downregulating expression of S100A4 and TGF $\beta$ 1 in CBDL rats. \* $p < 0.05$  and \*\* $p < 0.005$  compared to vehicle treated CBDL rats.

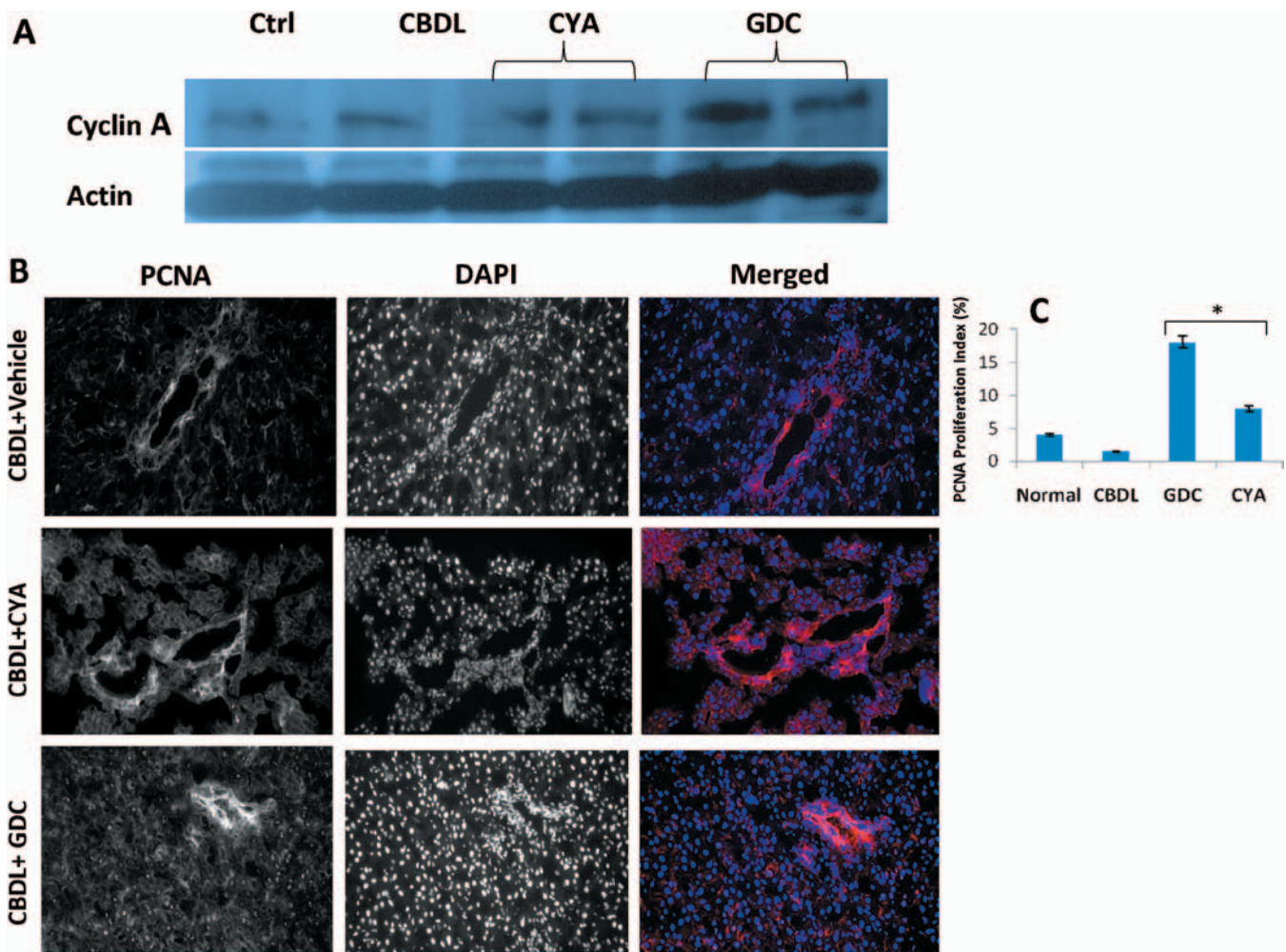


Figure 4. Effect of Smo inhibitors on cell proliferation in rat livers. (A) Immunoblot analysis was performed on whole liver extracts for proliferation marker cyclin A. Expression of cyclin A was increased in Smo inhibitor treated CBDL rats compared with vehicle treated CBDL rats. Compared to CYA, GDC caused a greater increase in expression of cyclin A. (B) Seven days after the CBDL, fresh frozen liver tissues were immunofluorescence stained for PCNA followed by staining for DAPI. Both separate panels (black and white images) and merged image (color) are shown. (C) The percentage of PCNA-positive nuclei to total nuclei at X100 magnification was quantitated using digital image analysis and is shown as proliferation index. The mean PCNA index was  $1.32\% \pm 1.37\%$ , with the highest proliferative rate recorded being 12.3% in GDC-treated group,  $*p < 0.05$ .

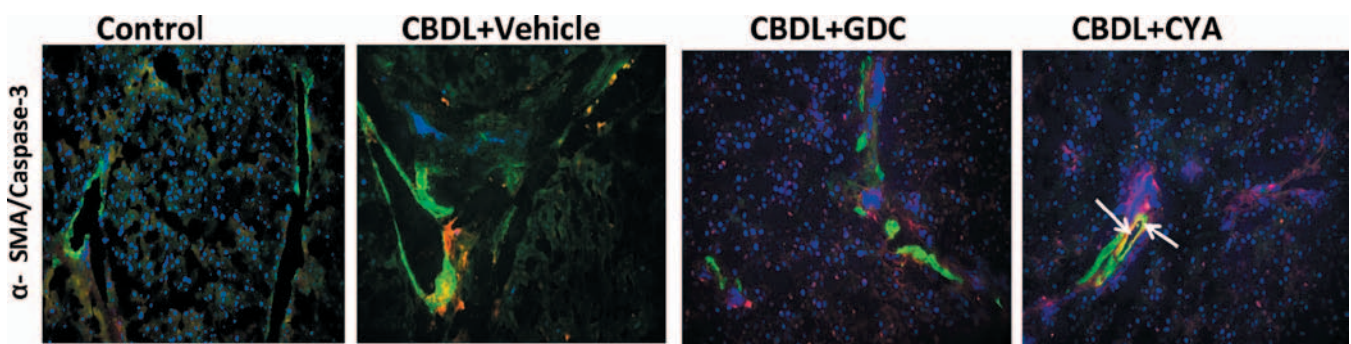


Figure 5. Effect of Smo inhibitors on HSC apoptosis in rat livers. Tissue sections were co-labeled with anti  $\alpha$ -smooth muscle actin ( $\alpha$ -SMA), marker for activated HSCs, and anti caspase-3. Double immunostaining using anti  $\alpha$ -SMA (green) and anti caspase 3 (red) showed enhanced merging (yellow, indicated by white arrows) in CYA-treated CBDL rats, indicating that the treatment resulted in caspase-3 expression in activated HSC cells *in vivo*. Little or no caspase-3 co-localization was observed in GDC-treated liver samples.

### Effect of SMO inhibitors on apoptosis

Activation of HSCs is a significant step that could lead to liver fibrosis. Therefore, to confirm that Smo inhibitors

enhance activated HSC apoptosis following CBDL,  $\alpha$ -SMA (marker for activated HSCs) and caspase-3 was measured in liver sections (Figure 5). Cells that were

positive for  $\alpha$ -SMA showed green and caspase-3 staining appeared red under fluorescence. Dual labeled cells appear as yellow in the field. As can be seen, while GDC treatment shows overall reduction in  $\alpha$ -SMA staining, no caspase-3 positive cells are visible. This is in contrast to CYA-treated specimen where extensive, all round yellow staining (white arrows) is clearly visible in the linings of bile ducts and portal tracts, suggesting that cells positive for  $\alpha$ -SMA expression were also expressing enhanced levels of caspase-3.

### SMO inhibitors reduce activation of HSCs in CBDL rats

Effect of Smo inhibitors on HSC activation was determined *in vivo*. Increased expression of  $\alpha$ -SMA is a widely accepted indicator of myofibroblast activation. After 1 week of CBDL,  $\alpha$ -SMA gene expression was markedly increased in vehicle-dosed CBDL rats compared with sham controls (Figure 6A). However, transcript levels were significantly decreased in CYA and GDC-treated rats compared with vehicle treated CBDL animals and GDC was more effective in downregulating gene expression of  $\alpha$ -SMA. This decrease in mRNA expression was matched by a decrease in hepatic  $\alpha$ -SMA protein expression assessed by Western blot analysis of whole liver tissue (Figure 6B). Immunofluorescence staining for  $\alpha$ -SMA in rat liver sections (Figure 6C) demonstrates extensive green staining in CBDL specimen. Treatment with Smo inhibitors was effective in ameliorating  $\alpha$ -SMA protein expression. These data indicate that Hh-mediated activation of HSCs *in vivo* is a central mechanism underlying hepatic fibrosis, and Smo inhibitors can effectively attenuate HSC activation, thereby preventing early fibrosis. Using double immunolabeling with digital image processing for simultaneous demonstration of CK-19 and  $\alpha$ -SMA in CBDL animals, we could identify cells in periductular regions co-expressing CK-19 (marker for cholangiocytes, red panel) and  $\alpha$ -SMA (EMT marker, green panel) (Figure 6D). These data indicate that in addition to HSCs, proliferating cholangiocytes mature into myofibroblasts expressing  $\alpha$ -SMA following CBDL injury. An arrow on the merged panel shows the extent of EMT undergone by the cholangiocytes in the CBDL livers.

### SMO inhibitors reduce expression of profibrogenic genes and attenuate early liver fibrosis

Type 1 collagen is a major regulator of ECM deposition in liver fibrosis. The effect of CYA and GDC on collagen deposition in CBDL rats was determined. Treatment with CYA and GDC significantly reduced the expression of type  $\alpha$ (1) collagen transcript as determined by real-time PCR (Figure 7A). While both GDC and CYA reduced total collagen, as determined by measuring hepatic hydroxyproline (Figure 7B), and protein expression of  $\alpha$ (1) collagen (Figure 7C), no statistical difference in their efficacy was observed. To explore the functional role of Smo inhibitors on CBDL induced fibrosis, the extent of liver fibrosis

using picrosirius red and Masson trichrome staining was carried out. After 1 week of CBDL, significant fibrosis was present in periportal and portal tracts (Figure 7D). Treatment with CYA and GDC significantly reduced the extent of bridging fibrosis with GDC being more effective, as indicated by an overall decrease in immunostaining.

## Discussion

Hepatic fibrosis leading to cirrhosis is associated with high morbidity and mortality in millions of people worldwide (Jemal et al., 2007; Rojkind & Martinez-Palomo, 1976). This highlights the urgent need to both increase our understanding of the mechanisms of liver fibrogenesis and to develop novel therapies to arrest or reverse the fibrotic process as even advance fibrosis is reversible (Soriano et al., 2006; Arthur, 2002). Preclinical studies have identified many potential therapies for fibrosis. These include inhibition of collagen synthesis, interruption of matrix deposition, stimulation of matrix degradation, modulation of HSC activation, or induction of HSC apoptosis (Fratto et al., 2011).

One of the strategies used in our laboratory and elsewhere is the targeting of collagen synthesis, since liver fibrosis results from the overproduction of type I collagen by fibrogenic cells. Transcription inhibition of type  $\alpha$ (I) collagen is expected to prevent fibrosis. We have previously shown that antiparallel phosphorothioate triplex forming oligonucleotides (TFO) specific for  $\alpha$ 1(I) collagen inhibit transcription in immortalized rat HSC-T6 cells in culture (Ye et al., 2007) and alleviate experimental fibrosis in rats subjected to CBDL or dimethylnitrosamine injections. Administration of TFO against  $\alpha$ 1(I) collagen decreased liver injury, inflammation, and attenuated fibrosis *in vivo*. The TFO approach, however, has some limitations, which reduce its overall effectiveness. For one, they can only bind to purine-rich target strands, thereby limiting the choice of endogenous gene target sites to polypurine-polypyrimidine stretches in duplex DNA. Moreover, TFO being a polypurine forms G quartet and requires a nuclear translocation for triplex formation with genomic DNA, which further limits its clinical applications (Uil et al., 2003). TGF- $\beta$ 1 is a profibrogenic cytokine that activates HSCs and induces EMT (Ischenko et al., 2008; Kisseleva and Brenner, 2011). In our previous studies, siRNA and shRNA targeting TGF- $\beta$ 1 can efficiently silence gene expression, which also resulted in decreased collagen synthesis (Yang and Mahato, 2011; Cheng et al., 2009). The siRNA approach too has some significant shortcomings, including the lack of efficient delivery systems, off target effects and poor *in vivo* stability, all of which hinder its translation into clinic (De Paula et al., 2007).

Liver regeneration involves Hh signaling and there is an increase in hepatic Hh activity following CBDL in rats and in patients diagnosed with primary biliary cirrhosis (Omenetti et al., 2008; Thayer et al., 2003). Dysregulation of Hh signaling plays a pivotal role in modulating liver injury and initiation

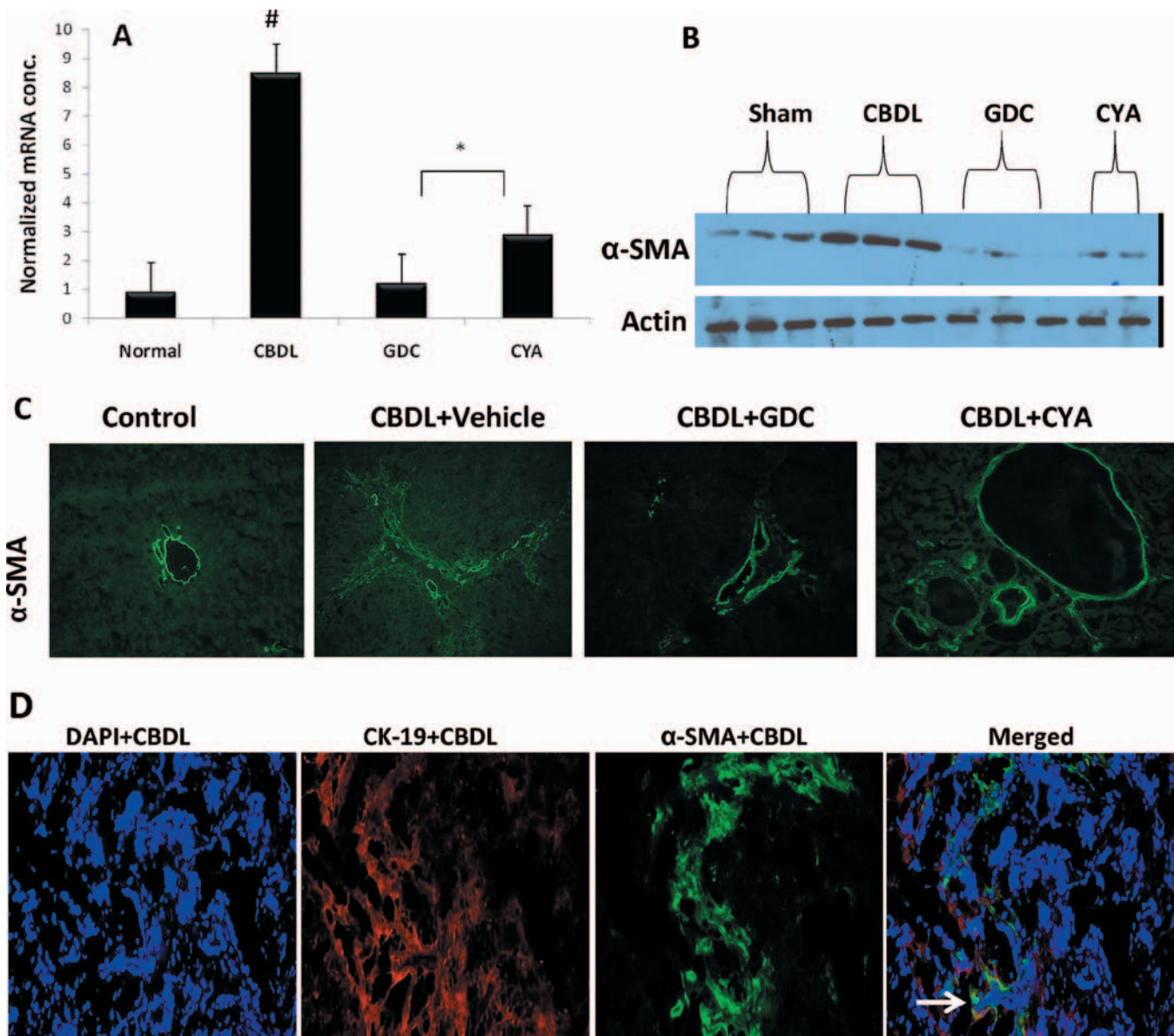


Figure 6. Smo inhibitors attenuate  $\alpha$ -SMA expression. (A) Gene expression measured by real-time RT-PCR; Protein expression determined by (B) Western blotting; and (C) Immunofluorescence staining.  $**p < 0.005$  compared to vehicle treated CBDL group. CBDL liver specimen showed higher  $\alpha$ -SMA gene and protein expression with greatest immunofluorescence staining observed in and around bile ducts. GDC treatment was more effective than CYA in reducing both protein and mRNA expression. (D) Immunofluorescence labeling of CBDL liver tissues with CK-19 (red) and  $\alpha$ -SMA (green) colocalized (yellow) in periportal areas (arrow).

of EMT that accelerates the induction of fibrosis (Omenetti et al., 2007; Cheng et al., 2008). However, the mechanisms of Hh signaling in hepatic cells are still being investigated. Following hepatic damage of various etiologies, HSCs get activated into ECM-secreting myofibroblasts (Friedman, 2008; Fernandez-del Castillo et al., 2003). In addition, influx of bone marrow-derived fibrocytes as well as differentiation of monocytes into fibrocytes in the damaged liver tissue results in the transformation of cholangiocytes and hepatocytes into myofibroblasts through EMT, in which epithelial cells lose their phenotypic characteristics and acquire typical features of mesenchymal cells such as fibroblasts (Zeisberg et al., 2007). To understand the mechanisms through which Hh signaling is involved in early liver fibrosis, as well as the

role of activated HSCs, we used two potent inhibitors of Hh signaling. CYA and GDC were given systemically to CBDL rats. Several studies have previously utilized CYA to treat liver cells, including primary HSCs *in vitro* (Choi et al., 2010a, Choi et al., 2010b). Previous work in our laboratory on treatment IR injury and CBDL rats subjected to IR injury with CYA ameliorates liver injury and prevent late fibrotic events (Pratap et al., 2010; Pratap et al., 2011). In spite of its efficacy in preventing liver fibrosis, CYA is highly insoluble in aqueous media and is acid-labile, which hampers its clinical potential (Tremblay et al., 2008). As we wanted to test the potential of an Hh inhibitor with enhanced *in vivo* stability and bioavailability, we utilized GDC, a small molecule inhibitor of Hh signaling (Rudin et al., 2009) for ameliorating early liver fibrosis in CBDL rats.

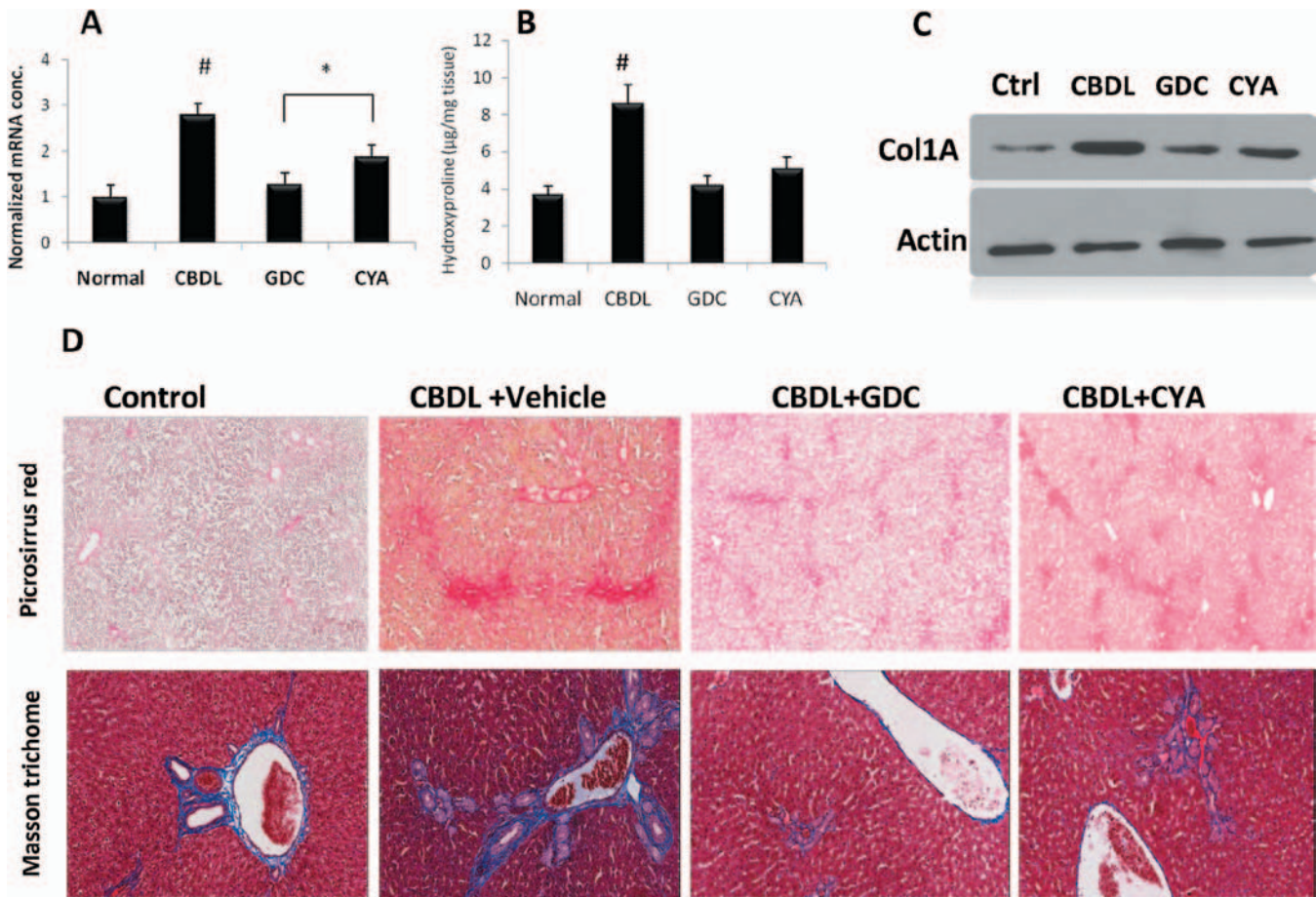


Figure 7. Smo inhibitors reduce collagen deposition and liver fibrosis. Treatment with CYA and GDC reduced (A) mRNA transcript as measured by real-time RT-PCR; (B) total collagen measured by hydroxyproline assay and (C)  $\alpha$  (1) collagen measured by Western blot in rat liver tissues.  $*p < 0.05$  compared to vehicle treated CBDL rat livers. Panel D indicates total collagen deposition in rat liver sections, as measured by picrosirius red and masson trichome staining. Dark blue staining with masson trichome indicates increased collagen deposition in CBDL livers. Both CYA and GDC effectively reduced collagen gene and protein expression in CBDL livers compared to vehicle treatment.

Vehicle treated rats subjected to 7 days of CBDL showed marked increase in liver size and presented a grainy texture with an overall patchy appearance and fibrous morphology (Figure 1A, top panels). Morphometric analysis of liver sections from vehicle treated CBDL rats showed marked increase in tissue damage as evinced by increased ballooning and large darkly stained necrotic regions indicated by arrows (Figure 1A, bottom panels). In addition, liver function markers such as serum AST, ALT and bilirubin were significantly upregulated compared to CYA and GDC-treated rats (Figure 1B). In both treatment groups, systemic treatment with CYA and GDC at 10 and 5 mg/kg, respectively, for 7 days resulted in the restoration of gross morphology features as well as restoration of liver functions, as shown by a decrease in the levels of serum bilirubin and liver function enzymes ALT and AST. Taken together, it is clear that even early fibrosis can result in tissue damage and impaired function of the liver. These findings confirm our hypothesis that liver injury resulting from CBDL surgery can be characterized as early as 7 days and systemic treatment with GDC at half-dose is as effective as CYA in ameliorating liver injury and restoring liver function.

Consistent with previously published reports (Omenetti et al., 2008; Hirose et al., 2009; Syn et al., 2009), the present study demonstrates increased Hh pathway expression in CBDL rats, as measured by and real-time RT-PCR and immunofluorescence (Figure 2A and 2B, respectively). EMT has been shown to play a vital role in the development of liver fibrosis (Xia et al., 2006). A decrease in the hepatic myofibroblast activation and biliary fibrosis was also observed when EMT was blocked by hepatocyte growth factor (Xia et al., 2006). As shown in Figure 3, expression of mesenchymal EMT markers such as S100A4 (Lo et al., 2011), TGF- $\beta$ 1 and  $\alpha$ -SMA was increased in CBDL rats, while that of E-cadherin, a known epithelial marker (Nierhoff et al., 2005) was significantly downregulated. Following treatment with CYA and GDC, expression of E-cadherin was restored while mesenchymal markers were significantly attenuated, suggesting that treatment with CYA and GDC prevents EMT and subsequent liver fibrosis.

Hh signaling has been associated with maintaining cellular proliferation (Yauch et al., 2008). CYA significantly inhibited proliferation and induced apoptosis of malignant hepatoma carcinoma cells as well as islet

tumor cells (Fendrich et al., 2011). In this study, CBDL rats treated with GDC and CYA showed enhanced proliferation as determined by Western blot for cyclin A (Figure 4A), a known maker for cell cycle progression and proliferation (Strand et al., 2012). To ascertain whether cells were proliferating as a result of drug treatment, immunofluorescence staining for PCNA was carried out. The data demonstrate a significant increase in PCNA positive cells in sections from CYA and GDC-treated rat livers (Figure 4B and 4C). While this may be in contrast to the available evidence in cancer cells treated with CYA, increased hepatocyte proliferation may actually be the healing mechanism through which the liver regenerates hepatocytes to replace the ones that perished as a result of CBDL injury and associated cytotoxic events initiated by activated HSCs and cholangiocytes. In several systems, Hh pathway can suppress apoptosis via transcriptional upregulation of inhibitors of both the extrinsic and intrinsic apoptotic pathways (Pratap et al., 2011) and is thus responsible for cell survival and proliferation. Another study demonstrated that co-treatment with CYA significantly increased the percentage of resistant cancer cells undergoing cell death and apoptosis (Delhaye et al., 1996). Our *in vivo* data are thus in accordance with these findings. Rat liver sections dual-stained with  $\alpha$ -SMA (activated HSC/EMT marker) and caspase-3 (apoptosis marker) indicate high levels of their co-localization in CYA-treated CBDL specimen and not in GDC-treated ones, suggesting that CYA is preferentially causing apoptosis of activated HSC cells (Figure 5).

In addition to HSCs, other cell types, including hepatocytes and bile ductular cells (cholangiocytes) produce Hh signaling ligands in response to liver injury. Injured mature hepatocytes, though non-responsive to Hh signaling, will release Hh ligands in the microenvironment, thereby activating nearby HSCs, which in turn overproduce ECM (Jung et al., 2010; Chen et al., 2002). In contrast, cholangiocytes not only produce Hh ligands but are also responsive to their effects (Witek et al., 2009). Regardless of the cell type involved in overproducing Hh ligands, HSCs are the major population responsible for liver repair and collagen production (Friedman, 1993; Moreira, 2007; Dooley et al., 2003). Furthermore,  $\alpha$ -SMA expression *in vivo* is a reliable marker of HSC activation prior to the deposition of fibrous tissue following liver injury and may be used to identify the earliest stages of hepatic fibrosis and monitoring the efficacy of the therapy (Carpino et al., 2005). Figure 6A and 6B shows increased expression of  $\alpha$ -SMA gene and protein, respectively in vehicle treated CBDL rat livers. Immunofluorescence staining of liver specimens from vehicle treated CBDL rats (Figure 6C) showed extensive  $\alpha$ -SMA expression (green fluorescence) with greatest staining in and around bile and portal ducts. Involvement of more than one cell type in etiology of CBDL-mediated liver fibrosis is supported by the dual staining of CBDL liver sections with CK-19 and  $\alpha$ -SMA, markers for cholangiocytes and EMT, respectively (Figure 6D). Dual-stained cells

are proliferating cholangiocytes that are maturing into  $\alpha$ -SMA expressing myofibroblasts. Treatment with GDC and CYA reduced both protein and mRNA expression in CBDL livers, suggesting that while liver injury resulted in the activation of HSCs, inhibition of Hh signaling could prevent this mechanism. Taken together, the data confirmed the involvement of EMT in HSC and cholangiocyte activation leading to liver fibrosis.

The principal finding of this study is the antifibrotic effect of Smo inhibitor GDC, suggesting its potential for treating early liver fibrosis. A decrease in the deposition of type  $\alpha$ 1(I) collagen was observed by real-time PCR (Figure 7A), hydroxyproline assay (Figure 7B) and Western blot (Figure 7C). Morphometric analyses also indicate an increase in collagen levels in CBDL rats, which was ameliorated following treatment with CYA and GDC (Figure 7D). As drug treatment was started immediately after the induction of CBDL, this study further suggests that the early treatment of hepatic fibrosis with Smo inhibitors such as GDC and CYA can reduce collagen deposition by downregulating Hh signaling in the liver and preventing hepatic cells from undergoing EMT.

The results of this study pertain to the ability of SMO inhibitors to modulate cholestatic liver injury leading to decreased liver fibrosis and improved tissue architecture, including a decrease in bile infarcts. It has been suggested that bile duct proliferation and bile infarcts may be caused by the toxic action of retained bile constituents that are absorbed into the blood from the obstructed biliary system, or a direct action on the liver (Shibayama, 1990). Furthermore, the growth of immature bile ductular cells in culture is regulated by Hh ligands, and Hh-pathway activity increases after CBDL (Omenetti et al., 2008). We have shown previously that preconditioning of cholestatic liver with CYA reduces the histological damage and serum liver injury markers resulting from IR injury. Significantly, untreated livers had increased neutrophil recruitment, lipid peroxidation, and pro-inflammatory cytokines, such as TNF- $\alpha$  and IL-1 $\beta$ , which resulted in increased cell death and cholangiocyte proliferation that accentuated liver injury and altered tissue architecture (Pratap et al., 2011). In the present study, it is possible that CBDL is causing similar molecular and cellular level changes as early as 7 days, which is a key finding. The direct or indirect effects of accumulating bile components causes not only inflammation but also result in the activation and increase in the number of HSCs and cholangiocytes, which in turn secrete not only Hh ligands but also  $\alpha$ -SMA and type 1 collagen causing fibrosis. This contention is supported by studies where elevated levels of bile acids stimulate ductal secretion and cholangiocyte proliferation (Alpini et al., 1999). Overall, this increase in Hh-mediated upregulation of bile-secreting cholangiocytes is responsible for the anatomical and tissue level changes in CBDL rat livers. Hepatoprotection by CYA and GDC is due to the blockade of aberrant endogenous Hh signaling, which reduces bile duct proliferation and inflammatory injury.

A decrease in the number of cholangiocytes is also likely to improve tissue morphology by reducing the amount of toxic bile being produced in the organ.

## Conclusions

In conclusion, Smo inhibitors has the potential to treat early liver fibrosis by reducing type  $\alpha 1(I)$  collagen synthesis leading to reduction in liver injury. GDC was better or equally effective in treating experimental liver fibrosis at half the dose of CYA. This indicates that GDC may be a new addition to the repertoire of small molecule drugs that can effectively treat liver fibrosis in a clinical setting.

## Declaration of interest

This work was partly supported by a grant from the National Institute of Health (to R.I.M.; project number: EB003922). The authors declare no competing financial interests.

## References

- Alpini G, Glaser SS, Ueno Y, Rodgers R, Phinzy JL, Francis H, Baiocchi L, Holcomb LA, Caligiuri A, LeSage GD. (1999). Bile acid feeding induces cholangiocyte proliferation and secretion: Evidence for bile acid-regulated ductal secretion. *Gastroenterology*, 116, 179–186.
- Arthur MJ. (2002). Reversibility of liver fibrosis and cirrhosis following treatment for hepatitis C. *Gastroenterology*, 122, 1525–1528.
- Asaoka Y, Kanai F, Ichimura T, Tateishi K, Tanaka Y, Ohta M, Seto M, Tada M, Ijichi H, Ikenoue T, Kawabe T, Isobe T, Yaffe MB, Omata M. (2010). Identification of a suppressive mechanism for Hedgehog signaling through a novel interaction of Gli with 14-3-3. *J Biol Chem*, 285, 4185–4194.
- Carpino G, Morini S, Ginanni Corradini S, Franchitto A, Merli M, Siciliano M, Gentili F, Onetti Muda A, Berloco P, Rossi M, Attili AF, Gaudio E. (2005).  $\alpha$ -SMA expression in hepatic stellate cells and quantitative analysis of hepatic fibrosis in cirrhosis and in recurrent chronic hepatitis after liver transplantation. *Dig Liver Dis*, 37, 349–356.
- Chen JK, Taipale J, Young KE, Maiti T, Beachy PA. (2002). Small molecule modulation of Smoothened activity. *Proc Natl Acad Sci USA*, 99, 14071–14076.
- Cheng F, Li Y, Feng L, Li S. (2008). Hepatic stellate cell activation and hepatic fibrosis induced by ischemia/reperfusion injury. *Transplant Proc*, 40, 2167–2170.
- Cheng K, Yang N, Mahato RI. (2009). TGF- $\beta$ 1 gene silencing for treating liver fibrosis. *Mol Pharm*, 6, 772–779.
- Choi SS, Syn WK, Karaca GE, Omenetti A, Moylan CA, Witek RP, Agboola KM, Jung Y, Michelotti GA, Diehl AM. (2010a). Leptin promotes the myofibroblastic phenotype in hepatic stellate cells by activating the hedgehog pathway. *J Biol Chem*, 285, 36551–36560.
- Choi SS, Witek RP, Yang L, Omenetti A, Syn WK, Moylan CA, Jung Y, Karaca GE, Teaberry VS, Pereira TA, Wang J, Ren XR, Diehl AM. (2010b). Activation of Rac1 promotes hedgehog-mediated acquisition of the myofibroblastic phenotype in rat and human hepatic stellate cells. *Hepatology*, 52, 278–290.
- De Paula D, Bentley MV, Mahato RI. (2007). Hydrophobization and bioconjugation for enhanced siRNA delivery and targeting. *RNA*, 13, 431–456.
- Delhaye M, Louis H, Degraef C, Le Moine O, Devière J, Gulbis B, Jacobovitz D, Adler M, Galand P. (1996). Relationship between hepatocyte proliferative activity and liver functional reserve in human cirrhosis. *Hepatology*, 23, 1003–1011.
- Dooley S, Hamzavi J, Bretkopf K, Wiercinska E, Said HM, Lorenzen J, Ten Dijke P, Gressner AM. (2003). Smad7 prevents activation of hepatic stellate cells and liver fibrosis in rats. *Gastroenterology*, 125, 178–191.
- Dormoy V, Danilin S, Lindner V, Thomas L, Rothhut S, Coquard C, Helwig JJ, Jacqmin D, Lang H, Massfelder T. (2009). The sonic hedgehog signaling pathway is reactivated in human renal cell carcinoma and plays orchestral role in tumor growth. *Mol Cancer*, 8, 123.
- Ezure T, Sakamoto T, Tsuji H, Lunz JG 3rd, Murase N, Fung JJ, Demetris AJ. (2000). The development and compensation of biliary cirrhosis in interleukin-6-deficient mice. *Am J Pathol*, 156, 1627–1639.
- Fang JW, Bird GL, Nakamura T, Davis GL, Lau JY. (1994). Hepatocyte proliferation as an indicator of outcome in acute alcoholic hepatitis. *Lancet*, 343, 820–823.
- Fendrich V, Rehm J, Waldmann J, Buchholz M, Christofori G, Lauth M, Slater EP, Bartsch DK. (2011). Hedgehog inhibition with cyclopamine represses tumor growth and prolongs survival in a transgenic mouse model of islet cell tumors. *Ann Surg*, 253, 546–552.
- Fernández-del Castillo C, Targarona J, Thayer SP, Rattner DW, Brugge WR, Warshaw AL. (2003). Incidental pancreatic cysts: Clinicopathologic characteristics and comparison with symptomatic patients. *Arch Surg*, 138, 427–3; discussion 433.
- Fratto ME, Santini D, Vincenzi B, Silvestris N, Azzariti A, Tommasi S, Zoccoli A, Galluzzo S, Maiello E, Colucci G, Tonini G. (2011). Targeting EGFR in bilio-pancreatic and liver carcinoma. *Front Biosci (Schol Ed)*, 3, 16–22.
- Friedman SL. (1993). Seminars in medicine of the Beth Israel Hospital, Boston. The cellular basis of hepatic fibrosis. Mechanisms and treatment strategies. *N Engl J Med*, 328, 1828–1835.
- Friedman SL. (2008). Hepatic stellate cells: Protean, multifunctional, and enigmatic cells of the liver. *Physiol Rev*, 88, 125–172.
- Hirose Y, Itoh T, Miyajima A. (2009). Hedgehog signal activation coordinates proliferation and differentiation of fetal liver progenitor cells. *Exp Cell Res*, 315, 2648–2657.
- Hooper JE, Scott MP. (2005). Communicating with Hedgehogs. *Nat Rev Mol Cell Biol*, 6, 306–317.
- Ischenko I, Camaj P, Seeliger H, Kleespies A, Guba M, De Toni EN, Schwarz B, Graeb C, Eichhorn ME, Jauch KW, Bruns CJ. (2008). Inhibition of Src tyrosine kinase reverts chemoresistance toward 5-fluorouracil in human pancreatic carcinoma cells: An involvement of epidermal growth factor receptor signaling. *Oncogene*, 27, 7212–7222.
- Jemal A, Siegel R, Ward E, Murray T, Xu J, Thun MJ. (2007). Cancer statistics, 2007. *CA Cancer J Clin*, 57, 43–66.
- Jung Y, Witek RP, Syn WK, Choi SS, Omenetti A, Premont R, Guy CD, Diehl AM. (2010). Signals from dying hepatocytes trigger growth of liver progenitors. *Gut*, 59, 655–665.
- Kepek-Lenhart D, Chen LC, Morris SM Jr. (1996). Novel actions of aspirin and sodium salicylate: Discordant effects on nitric oxide synthesis and induction of nitric oxide synthase mRNA in a murine macrophage cell line. *J Leukoc Biol*, 59, 840–846.
- Kisseleva T, Brenner DA. (2011). Anti-fibrogenic strategies and the regression of fibrosis. *Best Pract Res Clin Gastroenterol*, 25, 305–317.
- Krull CE. (2010). Sonic Hedgehog gets another role. *Nat Neurosci*, 13, 6–7.
- Lo JF, Yu CC, Chiou SH, Huang CY, Jan CI, Lin SC, Liu CJ, Hu WY, Yu YH. (2011). The epithelial-mesenchymal transition mediator S100A4 maintains cancer-initiating cells in head and neck cancers. *Cancer Res*, 71, 1912–1923.
- Lorusso PM, Jimeno A, Dy G, Adjei A, Berlin J, Leichman L, Low JA, Colburn D, Chang I, Cheeti S, Jin JY, Graham RA. (2011). Pharmacokinetic dose-scheduling study of hedgehog pathway inhibitor vismodegib (GDC-0449) in patients with locally advanced or metastatic solid tumors. *Clin Cancer Res*, 17, 5774–5782.

- Marshall J. (2006). Clinical implications of the mechanism of epidermal growth factor receptor inhibitors. *Cancer*, 107, 1207–1218.
- Moreira RK. (2007). Hepatic stellate cells and liver fibrosis. *Arch Pathol Lab Med*, 131, 1728–1734.
- Nierhoff D, Ogawa A, Oertel M, Chen YQ, Shafritz DA. (2005). Purification and characterization of mouse fetal liver epithelial cells with high *in vivo* repopulation capacity. *Hepatology*, 42, 130–139.
- Omenetti A, Porrello A, Jung Y, Yang L, Popov Y, Choi SS, Witek RP, Alpini G, Venter J, Vandongen HM, Syn WK, Baroni GS, Benedetti A, Schuppan D, Diehl AM. (2008). Hedgehog signaling regulates epithelial-mesenchymal transition during biliary fibrosis in rodents and humans. *J Clin Invest*, 118, 3331–3342.
- Omenetti A, Yang L, Li YX, McCall SJ, Jung Y, Sicklick JK, Huang J, Choi S, Suzuki A, Diehl AM. (2007). Hedgehog-mediated mesenchymal-epithelial interactions modulate hepatic response to bile duct ligation. *Lab Invest*, 87, 499–514.
- Panakanti R, Pratap A, Yang N, Jackson JS, Mahato RI. (2010). Triplex forming oligonucleotides against type a1(I) collagen attenuates liver fibrosis induced by bile duct ligation. *Biochem Pharmacol*, 80, 1718–1726.
- Park J, Zhang JJ, Moro A, Kushida M, Wegner M, Kim PC. (2010). Regulation of Sox9 by Sonic Hedgehog (Shh) is essential for patterning and formation of tracheal cartilage. *Dev Dyn*, 239, 514–526.
- Pratap A, Panakanti R, Yang N, Eason JD, Mahato RI. (2010). Inhibition of endogenous hedgehog signaling protects against acute liver injury after ischemia reperfusion. *Pharm Res*, 27, 2492–2504.
- Pratap A, Panakanti R, Yang N, Lakshmi R, Modanlou KA, Eason JD, Mahato RI. (2011). Cyclopamine attenuates acute warm ischemia reperfusion injury in cholestatic rat liver: Hope for marginal livers. *Mol Pharm*, 8, 958–968.
- Rojkind M, Martinez-Palomo A. (1976). Increase in type I and type III collagens in human alcoholic liver cirrhosis. *Proc Natl Acad Sci USA*, 73, 539–543.
- Rudin CM, Hann CL, Laterra J, Yauch RL, Callahan CA, Fu L, Holcomb T, Stinson J, Gould SE, Coleman B, LoRusso PM, Von Hoff DD, de Sauvage FJ, Low JA. (2009). Treatment of medulloblastoma with hedgehog pathway inhibitor GDC-0449. *N Engl J Med*, 361, 1173–1178.
- Shibayama Y. (1990). Factors producing bile infarction and bile duct proliferation in biliary obstruction. *J Pathol*, 160, 57–62.
- Sicklick JK, Li YX, Choi SS, Qi Y, Chen W, Bustamante M, Huang J, Zdanowicz M, Camp T, Torbenson MS, Rojkind M, Diehl AM. (2005). Role for hedgehog signaling in hepatic stellate cell activation and viability. *Lab Invest*, 85, 1368–1380.
- Singh S, Chitkara D, Mehrazin R, Behrman SW, Wake RW, Mahato RI. (2012). Chemoresistance in Prostate Cancer Cells Is Regulated by miRNAs and Hedgehog Pathway. *PLoS ONE*, 7, e40021.
- Soriano V, Labarga P, Ruiz-Sancho A, Garcia-Samaniego J, Barreiro P. (2006). Regression of liver fibrosis in hepatitis C virus/HIV-co-infected patients after treatment with pegylated interferon plus ribavirin. *AIDS*, 20, 2225–2227.
- Strand C, Ahlin C, Bendahl PO, Fjällskog ML, Hedenfalk I, Malmström P, Fernö M. (2012). Combination of the proliferation marker cyclin A, histological grade, and estrogen receptor status in a new variable with high prognostic impact in breast cancer. *Breast Cancer Res Treat*, 131, 33–40.
- Syn WK, Jung Y, Omenetti A, Abdelmalek M, Guy CD, Yang L, Wang J, Witek RP, Fearing CM, Pereira TA, Teaberry V, Choi SS, Conde-Vancells J, Karaca GF, Diehl AM. (2009). Hedgehog-mediated epithelial-to-mesenchymal transition and fibrogenic repair in nonalcoholic fatty liver disease. *Gastroenterology*, 137, 1478–1488. e8.
- Thayer SP, di Magliano MP, Heiser PW, Nielsen CM, Roberts DJ, Lauwers GY, Qi YP, Gysin S, Fernández-del Castillo C, Yajnik V, Antoniu B, McMahon M, Warshaw AL, Hebrok M. (2003). Hedgehog is an early and late mediator of pancreatic cancer tumorigenesis. *Nature*, 425, 851–856.
- Tremblay MR, Nevalainen M, Nair SJ, Porter JR, Castro AC, Behnke ML, Yu LC, Hagel M, White K, Faia K, Grenier L, Campbell MJ, Cushing J, Woodward CN, Hoyt J, Foley MA, Read MA, Sydor JR, Tong JK, Palombella VJ, McGovern K, Adams J. (2008). Semisynthetic cyclopamine analogues as potent and orally bioavailable hedgehog pathway antagonists. *J Med Chem*, 51, 6646–6649.
- Uil TG, Haisma HJ, Rots MG. (2003). Therapeutic modulation of endogenous gene function by agents with designed DNA-sequence specificities. *Nucleic Acids Res*, 31, 6064–6078.
- Varnat F, Duquet A, Malerba M, Zbinden M, Mas C, Gervaz P, Ruiz i Altaba A. (2009). Human colon cancer epithelial cells harbour active HEDGEHOG-Gli1 signalling that is essential for tumour growth, recurrence, metastasis and stem cell survival and expansion. *EMBO Mol Med*, 1, 338–351.
- Wang K, Pan L, Che X, Cui D, Li C. (2010). Gli1 inhibition induces cell-cycle arrest and enhanced apoptosis in brain glioma cell lines. *J Neurooncol*, 98, 319–327.
- Witek RP, Yang L, Liu R, Jung Y, Omenetti A, Syn WK, Choi SS, Cheong Y, Fearing CM, Agboola KM, Chen W, Diehl AM. (2009). Liver cell-derived microparticles activate hedgehog signaling and alter gene expression in hepatic endothelial cells. *Gastroenterology*, 136, 320–330.e2.
- Xia JL, Dai C, Michalopoulos GK, Liu Y. (2006). Hepatocyte growth factor attenuates liver fibrosis induced by bile duct ligation. *Am J Pathol*, 168, 1500–1512.
- Yang N, Mahato RI. (2011). GFAP promoter-driven RNA interference on TGF- $\beta$ 1 to treat liver fibrosis. *Pharm Res*, 28, 752–761.
- Yauch RL, Gould SE, Scales SJ, Tang T, Tian H, Ahn CP, Marshall D, Fu L, Januario T, Kallop D, Nannini-Pepe M, Kotkow K, Marsters JC, Rubin LL, de Sauvage FJ. (2008). A paracrine requirement for hedgehog signalling in cancer. *Nature*, 455, 406–410.
- Ye Z, Guntaka RV, Mahato RI. (2007). Sequence-specific triple helix formation with genomic DNA. *Biochemistry*, 46, 11240–11252.
- Zeisberg M, Yang C, Martino M, Duncan MB, Rieder F, Tanjore H, Kalluri R. (2007). Fibroblasts derive from hepatocytes in liver fibrosis via epithelial to mesenchymal transition. *J Biol Chem*, 282, 23337–23347.